EXAFS and Density Functional Study of Gold(I) Thiosulfate Complex in Aqueous Solution

Richard A. Bryce,*,† John M. Charnock,‡ Richard A. D. Pattrick,§ and Alistair R. Lennie*,‡

School of Pharmacy & Pharmaceutical Sciences, University of Manchester, Oxford Road, Manchester, M13 9PL U.K., Daresbury Laboratory, Warrington, Cheshire, WA4 4AD U.K., and Department of Earth Sciences, University of Manchester, Oxford Road, Manchester, M13 9PL U.K.

Received: June 12, 2002; In Final Form: January 24, 2003

The gold thiosulfate complex, $Au(S_2O_3)_2^{3-}$, has been studied using extended X-ray absorption fine structure (EXAFS) spectroscopy and high level quantum mechanical calculations, which include the effect of aqueous solvent via a dielectric continuum model. EXAFS measurements on $Au(S_2O_3)_2^{3-}$ show gold coordinated by two sulfurs at 2.29 Å. Density functional calculations, incorporating the effect of solvent using the COSMO method, show the 2-fold S coordination of Au to be linear in geometry. This computational approach is further employed to examine the conformational potential energy surface of the complex in aqueous solution. As expected from the significant deviation (108°) between the calculated conformation in aqueous solution and the observed crystal structure, internal rotation about the S−Au−S axis is facile: calculation predicts a rotational barrier in solution of less than 3 kcal/mol. Calculated Au−S bond dissociation energies indicate a strong metal−S bond in aqueous solution. Lower solution stability of $Au(S_2O_3)_2^{3-}$ with respect to another thio gold complex, $Au(SH)_2^-$, is predicted in accord with measured overall stability constants. These calculations, together with our experimental observation that $Au(S_2O_3)_2^{3-}$ decomposes at 393 K, support the view that gold transport by the thiosulfate complex of Au(I) may be restricted to ambient and moderate temperatures. This contrasts with the Au(I) thiolate complex which can mobilize gold at elevated temperature and pressure.

1. Introduction

Understanding aqueous metal speciation is critical for development of models for metal cycling at the surface of the Earth and within its crust. Knowledge of these processes enhances thermodynamic and transport modeling of aqueous metals, and enables predictive studies of metal behavior in aqueous solution. The aqueous chemistry of a number of metals depends on the nature of metal−S complexation. The range of chemical and coordination behavior exhibited by such metal−S complexes leads to sulfide-rich reducing environments acting as either sources or sinks for these metals, which may include metals toxic to biota.

In this study, we explore aspects of Au−S aqueous chemistry. A number of experimental and theoretical studies have addressed the nature of aqueous Au−S transport, which is important for understanding Au cycling and Au ore formation.[1−3] Spectroscopic measurement of gold thiolate complexes is made difficult by very low dissolved concentrations of these species in sulfidic waters. In contrast to gold thiolate complexes, however, Au(I) forms extremely soluble complexes with thiosulfate.[2]

Thiosulfate shows versatile crystal chemical behavior.[4] Thiosulfate may crystallize as a discrete anion,[5] as in $MgS_2O_3{\cdot}6H_2O$, or ligand where coordination to the metal cation may be through S,[6,7] as in $NaAgS_2O_3{\cdot}H_2O$ and $Na_3Au(S_2O_3)_2{\cdot}2H_2O$, or through both S and O atoms[8] as in $Ni[SC(NH_2)_2)]_4S_2O_3{\cdot}H_2O$. The S−S bond length in thiosulfate varies depending on the nature of bonding to the adjacent cation: in $BaS_2O_3{\cdot}H_2O$, where thiosulfate is a discrete anion,[9] the S−S bond distance is 1.96 Å; by contrast, with a S−S distance of 2.07 Å in $Na_3[Au(S_2O_3)_2]{\cdot}2H_2O$, bonding to Au occurs through the outer sulfur.[7]

In hydrothermal systems, thiosulfate forms as a metastable product of sulfide or sulfur oxidation; hydrolysis of sulfur leads to steady-state concentrations of thiosulfate,[10] which may reach concentrations of up to 7×10^{-4} M in surficial geothermal waters.[11] Rapid turnover of thiosulfate may be catalyzed by heterogeneous reactions, such as oxidation to tetrathionate on pyrite surfaces.[12] In bacterial metabolic pathways involving sulfur, thiosulfate is a key intermediate during oxidative or reductive conversions between sulfur, sulfide, and sulfate.[13] Because thiosulfate is present in nature under such conditions, gold thiosulfate complexes have been proposed as sources of secondary enrichment of Au in ore supergene environments.[14]

Recent physicochemical studies of metal solubilities and speciation in sulfidic aqueous media have employed a variety of spectroscopic techniques to elucidate the nature of the solution species. X-ray absorption spectroscopy (XAS) and specifically extended X-ray absorption fine structure (EXAFS) spectroscopy are powerful methods for providing local structural information around the atom of interest. In this study, we employ EXAFS to probe the local structural environment of the $Au(S_2O_3)_2^{3-}$ complex. Although previous studies have used EXAFS to investigate Au−S bonding in solid compounds, to our knowledge this is the first study of aqueous Au−S inorganic complexes using X-ray absorption spectroscopy. We then extend our analysis from local structure to the global conformation and energetic stability of the $Au(S_2O_3)_2^{3-}$ complex, employing high level quantum mechanical calculations including the effect of

* Corresponding authors. E-mail: R.A.Bryce@man.ac.uk (telephone: 0161-275-8345; fax: 0161-275-+81) (R.A.B.). E-mail: A.Lennie@dl.ac.uk (A.R.L.).

† School of Pharmacy & Pharmaceutical Sciences, University of Manchester.

‡ Daresbury Laboratory.

§ Department of Earth Sciences, University of Manchester.

10.1021/jp021403j CCC: $25.00
Published on Web 03/15/2003

aqueous solvent via the dielectric continuum model, COSMO.[15] For comparison, the theoretical treatment is extended to the $Au(SH)_2^-$ species, another thio−Au(I) complex implicated in hydrothermal transport of gold.

2. Methods

2.1. Experimental Methods. Data were obtained at the SRS, CLRC Daresbury Laboratory, UK. The current varied between 150 and 250 mA in the 2 GeV storage ring. Station 16.5 was used to collect the L_{III} edge X-ray fluorescence spectra. This station has been designed as a state-of-the-art facility for ultradilute EXAFS, with focusing optics to optimize flux at the sample and a high count rate fluorescence detector. A Si(220) double crystal monochromator is employed, with the second crystal dynamically bent during scanning to achieve horizontal focus.

The monochromator was calibrated with a sample of solid $Na_3Au(S_2O_3)_2 \cdot 2H_2O$ diluted with boron nitride, the Au edge of which was measured at 11 930.4 eV. The X-ray adsorption data for the solid was collected in transmission mode using ion chambers filled with Ar and He so as to absorb 20% of the incident monochromatic beam at the Au L_{III} edge in the first ion chamber and 80% in the second ion chamber. A Pb collimator placed before the I_o detector reduced stray reflections following dynamic focusing. This collimation arrangement was retained for solution experiments.

Solution data were obtained using a spectroscopic cell developed for these experiments. The titanium cell, with PEEK windows, is backed with a titanium block containing cartridge heaters to allow internal heating.[16] Thermostatic control is achieved using a Eurotherm heating controller. The control thermocouple is located close to the cell fluid chamber to maintain the temperature within ±1 K of the desired temperature. Gold thiosulfate solutions (10 mM) were prepared by dissolving $Na_3Au(S_2O_3)_2 \cdot 2H_2O$ in deionized deaerated water.[7] This solution was introduced into the spectroscopic cell under nitrogen.

The cell was mounted with the front window angled at 45° to the incident X-ray beam. Solution data was collected in fluorescence mode, with measurements taken at 90° to the beam direction in plane position. The Ortec 30-element fluorescence detector is a high purity Ge solid-state detector array coupled to high count rate electronics. Count rates in excess of 200 kHz per channel are achieved without loss of linearity. For these measurements, between four and eight spectra were recorded and averaged for each sample to improve the EXAFS signal-to-noise ratio. Individual spectra to $k = 14$ Å^{-1} were collected in about 40 min at 298, 348, and 393 K. Above 410 K, the internal pressure of the cell fluid caused the PEEK windows to deform.

The L_{III} edge spectra were calibrated in the SRS program EXCALIB. The edge position of each spectrum was determined as being the maximum in the first derivative of the fluorescence signal. Data were background subtracted using the SRS program EXBACK. EXAFS data analyses were performed using curved wave theory, including multiple scattering for the solid, in the program EXCURV98.[17−19] Phase shifts were calculated ab initio using Hedin−Lundqvist exchange potentials and von Barth ground-state potentials. For each spectrum, the parameters refined were E_f, an energy offset, and for each shell, the distance from the central Au and a Debye−Waller factor which represents both static and thermal disorder. The fit index R is defined elsewhere.[20] The number of atoms in each shell was chosen as the integer value which gave the best fit.

2.2. Computational Methods. Quantum mechanical calculations on systems involving third row elements present a challenge in terms of incorporating a large number of electrons and relativistic effects. Consequently, we describe the behavior of Au at two levels of theory: the relativistic one-electron effective core potential of Hay and Wadt[21] to model the chemically inert core electrons of Au, in conjunction with the double-ζ D95 basis set[22] to describe the valence electrons of Au. This combined basis is denoted as LANL2DZ. Although originally parametrized for use with the HF method, these potentials have also been used effectively[23] in combination with the B3LYP density functional[24,25] that we employ here. This functional combines the three-parameter HF/DFT hybrid exchange functional of Becke (B3)[24] with the dynamical correlation functional of Lee, Yang, and Parr (LYP).[25] Alternatively, we describe Au using the relativistic pseudopotential of Andrae et al.[26] with a contracted [6s5p3d] valence basis set, augmented by two diffuse functions of exponents 0.001 and 0.003, after an approach adopted in a study of gold species[27] including Au_2^-. We subsequently denote this larger metal basis as SD+. Both pseudopotential methods treat the Au core as [Xe]$4f^{14}$. On thiosulfate and thiolate, we employ two split-valence bases: the 6-31+G* basis[28] and the more flexible 6-311++G(2df) basis.[29] Optimal structures were obtained without symmetry constraints using analytic gradient methods. In vacuo stationary points were characterized as minima. Dissociation of the complexes to discrete ligands and metal was considered. Bond dissociation energies were computed as one-half of the energy required for dissociation of the gold(I) complex into the three isolated species (metal and two ligands). For example, for the gold(I) thiosulfate complex, dissociation is given as

$$Au(S_2O_3)_2^{3-} \rightarrow Au^+ + 2S_2O_3^{2-} \qquad (1)$$

Basis set superposition error (BSSE) was calculated using the counterpoise approach.[30] Zero-point vibrational energy and thermal contributions to bond dissociation energies and free energies of dissociation were obtained from normal mode vibrational frequency calculations using standard statistical mechanical methods.[31] For computational tractability, in vacuo second derivative calculations were performed at the B3LYP/LANL2DZ/6-31+G*//B3LYP/LANL2DZ/6-31+G* level of theory.

The effect of aqueous solvent on structure and energetics of the complex was studied using the conductor-like screening model (COSMO).[15] In this dielectric continuum solvent model, charges centered on surface elements, induced by the electrostatic potential of the solute, are determined self-consistently. A dielectric of 78.4 was employed and 60 tessera per sphere for cavity tesselation. Nonelectrostatic contributions include short-range dispersion−repulsion and cavity formation contributions to the solvation free energy, calculated using methods outlined elsewhere.[32,33] Here, dispersion−repulsion interactions were calculated for Au, S, O, and H employing the UFF force field parameters.[34] The united atom for Hartree−Fock (UAHF) procedure[35] was used to assign radii of ligand atoms for the calculation of electrostatic free energies in solution. To obtain an accurate Au^+ radius, we initially determined a value of 2.16 Å from volume integration of the 10^{-3} au isodensity envelope around the cation, leading to a free energy of solvation of −57.5 kcal/mol at the COSMO/B3LYP/LANL2DZ level, including nonelectrostatic contributions. Although an experimental value of ΔG_{solv} for Au(I) is unavailable, Cs(I) and Tl(I) have measured ΔG_{solv} of −60 and −72 kcal/mol,[36] respectively, suggesting the solvation energy is underestimated for Au(I). As a result, we

TABLE 1: EXAFS Analyses of Gold Bisthiosulfate solid ($Na_3Au(S_2O_3)_2 \cdot 2H_2O$) Obtained by X-ray Absorption on Station 16.5, Daresbury Laboratory[a,b]

sample	scatterer	N	r (Å)	$2\sigma^2$ (Å^2)	R-factor	ref
$Na_3Au(S_2O_3)_2 \cdot 2H_2O$	S	2	2.28	0.006	25.8	this work
	Au	1	3.30	0.025		
	S	2	3.41	0.023		
$Au(S_2O_3)_2^{3-}$ complexes in aq soln						
298 K	S	2	2.29	0.008	28.8	this work
348 K	S	2	2.30	0.004	37.6	this work
$Au_2\{S_2CN(C_2H_4OMe)_2\}_2$						
	S	2	2.289, 2.292			40
	S	2	2.296, 2.300			40

[a] The Au L_{III} edge position was measured at 11 930.4 eV. Transmission measurements of this solid diluted in boron nitride were taken on Station 16.5 with the curved geometry of the monochromator focusing crystal applied. One scan was taken at room temperature for transmission. For comparison, radial distances from Au in $Na_3Au(S_2O_3)_2 \cdot 2H_2O$ calculated from the X-ray data[39] are as follows: S, 2.272 Å; S, 2.281 Å; Au, 3.301 Å; S, 3.411 Å; S, 3.421 Å. [b] N is the number of scatterers in the shell ± 20%; r is the absorber−scatterer distance ± 0.02 Å; $2\sigma^2$ is the Debye−Waller factor ± 20%; R is a least-squared residual, showing the goodness of fit.

adopted an alternative value of 1.66 Å using the Bondi radius.[37] This radius gave a calculated free energy of solvation of −80.3 kcal/mol at the COSMO/B3LYP/LANL2DZ level including nonelectrostatic contributions (−80.1 kcal/mol at the COSMO/B3LYP/SD+ level) and was adopted for subsequent calculations in this work. For $S_2O_3^{2-}$ in solution, a ΔG_{solv} of −210.6 kcal/mol was calculated at the COSMO/B3LYP/6-31+G* level of theory, which is comparable to an experimental ΔG_{solv} of −258 kcal/mol[36] for the more compact SO_4^{2-}.

All calculations were performed using the Gaussian 98 suite of programs.[38] Calculated aqueous solution stationary structures are provided as Supporting Information.

3. Results

Solid $Na_3Au(S_2O_3)_2 \cdot 2H_2O$ was measured in one scan taken in transmission. Refined data are listed in Table 1, and the refinement is shown in Figure 1. First, second, and third shells visible in the EXAFS are fitted with Au and S. The peak in the Fourier transform at ca. 4.5 Å was fitted using multiple scattering from a linear S−Au−S unit. The major contributions to the multiple scattering are from paths through the central Au atom. For gold thiosulfate complexes in aqueous solution, four scans taken in fluorescence mode at each temperature were combined to improve the signal-to-noise ratio. The results of refinements of these data taken at 298 and 348 K are shown in Table 1 and Figure 2. Data were also collected at 393 K, but over successive scans they showed a continuous decrease in signal, providing unreliable data. Decomposition of the gold thiosulfate complex was observed at this temperature.

For quantum mechanical calculations of thio gold structure and energetics, it is first necessary to consider the most appropriate level of theory. A recent study[41] of the structures of Au(I) diatomics AuH and Au_2 found HF, MP2, and B3LYP methods to give low root-mean-square deviation from experiment for geometric parameters: B3LYP 3%, MP2 5%, and HF 5%. With respect to the ligand, HF,[42] B3LYP, and MP2 methods[43] have been used effectively with split-valence Gaussian bases to structurally characterize oxides of sulfur. To evaluate the most suitable level of theory at which to calculate energetics of the gold thiosulfate and thiolate complexes, the first ionization energy for Au was calculated (Table 2). Due to relativistic effects, the ionization energy for gold is anomalously high. However, the relativistic pseudopotential LANL2DZ combined with the B3LYP density functional leads to a calculated ionization energy of 9.42 eV (Table 2), giving very good agreement with the experimental value of 9.23 eV,[45] better than HF, MP2, or even the highly correlated CCSD(T) approach.

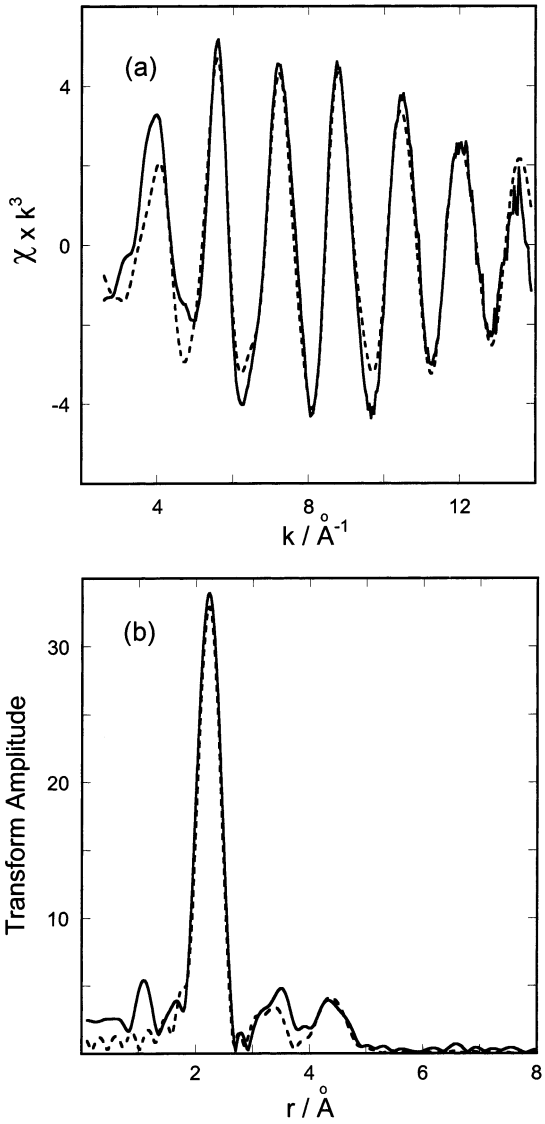

Figure 1. (a) Experimental EXAFS spectrum (solid line) and theoretical fit (broken line) of solid $Na_3Au(S_2O_3)_2 \cdot 2H_2O$. (b) Fourier transform of the spectrum (solid line) and fit (broken line) of solid $Na_3Au(S_2O_3)_2 \cdot 2H_2O$.

With the larger SD+ basis on Au, a similar B3LYP value of 9.44 eV is obtained (Table 2), suggesting a measure of convergence in this quantity with basis. The ability of B3LYP to accurately calculate ionization energies and electron affinities has been noted previously,[46,47] obtaining agreement to within

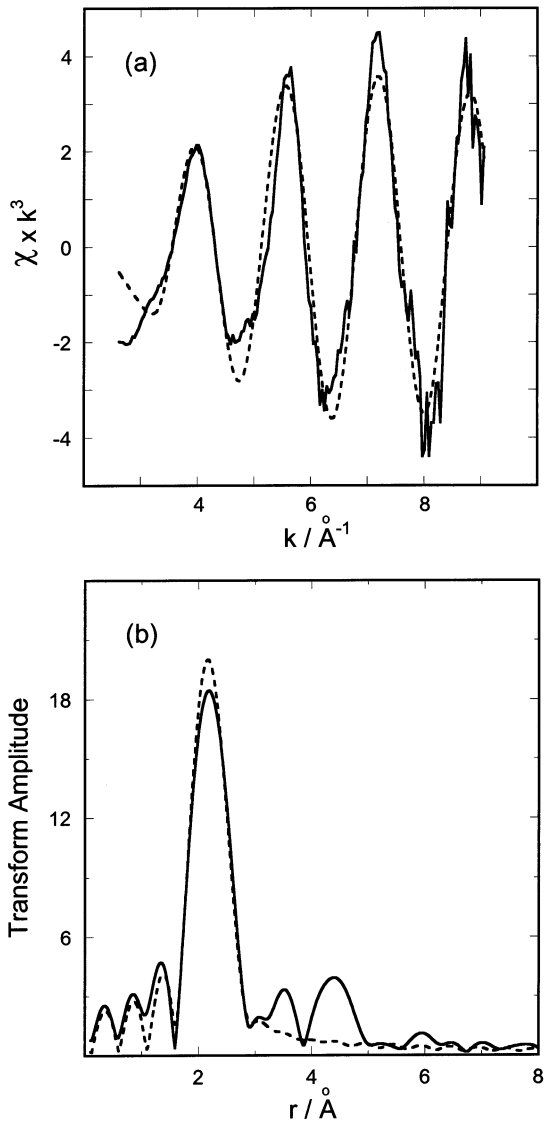

Figure 2. (a) Experimental EXAFS spectrum (solid line) and theoretical fit (broken line) of the gold thiosulfate solution complex at 298 K. (b) Fourier transform of the spectrum (solid line) and fit (broken line) of the gold thiosulfate solution complex at 298 K.

TABLE 2: First Ionization Energy (IE) of Au in Gas Phase

method	IE (eV)
HF[a]	7.77
HF[b]	7.70
BLYP[a]	9.49[c]
B3LYP[a]	9.42
B3LYP[b]	9.44
MP2[a]	8.18
MP2[b]	8.36
CCSD(T)[a]	8.26[c]
expt	9.23[d]

[a] Using LANL2DZ. [b] Using SD+. [c] Reference 44. [d] Reference 45.

0.13 eV for the electron affinity of F.[46] We therefore use the B3LYP density functional for calculations of gold thiosulfate and thiolate structure and energetics.

To subsequently test the energetic accuracy of the B3LYP density functional in combination with the reaction field solvent model, we calculate the reduction half-reaction energy at 298 K in aqueous solution for the Au(I)/Au(0) couple. Experimentally, the electrode potential has been measured as 1.69 V.[48] Correction of our calculated electrode potential at the COSMO/B3LYP/LANL2DZ level for the reference hydrogen electrode[49] gives a half-reaction energy of −133.8 kcal/mol, 7.6 kcal/mol less negative than the experimental value of −141.4 kcal/mol (Table 3). With the larger SD+ basis, agreement with experiment is modestly improved by 0.7 kcal/mol. Conversely, the magnitude of the gas-phase ionization energy of Au is overestimated, by 4.5 and 5.0 kcal/mol for B3LYP/LANL2DZ and B3LYP/SD+ levels, respectively (Table 3). The resulting difference of 12.1 and 11.9 kcal/mol for the two respective levels of theory may be attributed to the error arising from the continuum solvent model and is small, given neglect of explicit solvent interactions, in particular the two waters of the inner sphere complex with the gold cation.[50]

TABLE 3: Calculated Free Energies for Au(I) Reduction in Gas Phase, ΔG(gas), and Aqueous Solution via COSMO Solvent Model, ΔG(aq), Compared with Experimental Values[a]

method	reductive half-reaction	ΔG(gas)	ΔG(aq)
B3LYP/LANL2DZ	$Au^+ + e \rightarrow Au$	−217.3	−133.8
B3LYP/SD+	$Au^+ + e \rightarrow Au$	−217.8	−134.5
expt[b]	$Au^+ + e \rightarrow Au$	−212.8	−141.4

[a] Energies are in kcal/mol. [b] Experimental values from refs 45 and 48.

TABLE 4: Calculated Aqueous Solution Geometries of $Au(S_2O_3)_2^{3-}$ via COSMO and Comparison with Experiment[a]

coordinate	B3LYP/ LANL2DZ[b]	B3LYP/ SD+[b]	expt[c]	expt[d]
R(Au−S_1)	2.372	2.357	2.28, 2.27	2.29
R(S_1–S_2)	2.135	2.139	2.07, 2.05	
θ(S_1−Au−S_5)	179.7	179.6	176.5	
θ(Au−S_1−S_2)	104.3	104.8	103.6, 104.1	
φ(S_2−S_1−S_5−S_6)	178.1	175.2	67	

[a] Bond distances are in Å and angles in deg. [b] 6-31+G* basis applied to ligand atoms. [c] Crystallographic values.[39] [d] Distance from EXAFS at 298 K.

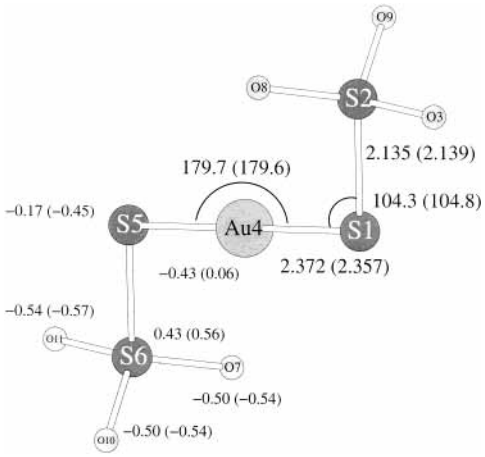

Figure 3. Optimal structure of $Au(S_2O_3)_2^{3-}$ at the COSMO/B3LYP/LANL2DZ/6-31+G* level of theory. COSMO/B3LYP/SD+/6-31+G* values are indicated in parentheses. Distances are in Å, angles in deg, and Mulliken charges (using 6-311++G(2df) basis on ligands) in e.

Calculated structures of the $Au(S_2O_3)_2^{3-}$ complex in aqueous solution are presented in Table 4, corresponding to the labeling scheme in Figure 3. These structures are compared with the EXAFS solution structure determined in this study, and with a crystal structure of the hydrate,[39] $Na_3Au(S_2O_3)_2 \cdot 2H_2O$. Minimum energy solution structures of a related thio gold(I) complex, $Au(SH)_2^-$, are presented for comparison in Table 5. In both the thiosulfate and thiolate complexes, we consider only

TABLE 5: Calculated Aqueous Solution Geometries of $Au(SH)_2^-$ via COSMO[a]

coordinate	B3LYP/LANL2DZ[b]	B3LYP/SD+[b]
$R(Au-S_1)$	2.371	2.355
$R(S_1-H_5)$	1.356	1.357
$\theta(S_1-Au-S_3)$	178.1	178.2
$\theta(Au-S_1-H_5)$	98.0	98.7
$\varphi(H_5-S_1-S_3-H_4)$	81.3	83.1

[a] Bond distances are in Å and angles in deg. [b] 6-31+G* basis applied to ligand atoms.

TABLE 6: Au−S Bond Dissociation Energy (ΔE) in $Au(S_2O_3)_2^{3-}$ Complex at COSMO/B3LYP Level of Theory with a Range of Metal and Ligand Basis (kcal/mol), Incorporating Basis Set Superposition Error (ΔE^{BSSE}) and Zero-Point Vibrational Effects (ΔE^0)

metal	ligand	ΔE[a]	ΔE^{BSSE}	ΔE^0
LANL2DZ	6-31+G*	53.0 (2.0)	52.2	51.4
LANL2DZ	6-311++G(2df)	55.4 (1.2)	54.6	54.0
SD+	6-31+G*	54.0 (2.0)	53.2	52.5
SD+	6-311++G(2df)	56.8 (2.8)	54.6	53.8

[a] Per ligand distortion energies in parentheses.

TABLE 7: Au−S Bond Dissociation Energy (ΔE) in $Au(SH)_2^-$ Complex at COSMO/B3LYP Level of Theory with a Range of Metal and Ligand Basis (kcal/mol), Incorporating Basis Set Superposition Error (ΔE^{BSSE}) and Zero-Point Vibrational Effects (ΔE^0)

metal	ligand	ΔE[a]	ΔE^{BSSE}	ΔE^0
LANL2DZ	6-31+G*	54.1 (0.2)	53.0	51.4
LANL2DZ	6-311++G(2df)	55.5 (0.2)	54.2	52.6
SD+	6-31+G*	55.6 (0.1)	54.4	52.7
SD+	6-311++G(2df)	57.1 (0.1)	55.9	54.2

[a] Per ligand distortion energies in parentheses.

TABLE 8: Free Energy of Dissociation of $Au(S_2O_3)_2^{3-}$ (ΔG_1) and $Au(SH)_2^-$ Complexes (ΔG_2) in Aqueous Solution at 298 K, at COSMO/B3LYP Level of Theory with a Range of Metal and Ligand Basis, Incorporating BSSE, Zero-Point and Thermal Contributions, and Corresponding Relative Dissociation Free Energy ($\Delta\Delta G$)[a]

metal	ligand	ΔG_1	ΔG_2	$\Delta\Delta G$
LANL2DZ	6-31+G*	96.6	100.0	3.4
LANL2DZ	6-311++G(2df)	101.4	102.4	1.0
SD+	6-31+G*	98.6	102.8	4.2
SD+	6-311++G(2df)	101.4	105.8	4.4
				5.4[b]

[a] All energies are in kcal/mol. [b] Experimental value from refs 1 and 14.

complexation to the metal via the S-atom. Au−S bond dissociation energies for $Au(S_2O_3)_2^{3-}$ and $Au(SH)_2^-$ complexes are presented in Tables 6 and 7, respectively, and corresponding total free energies of dissociation of the complexes in Table 8.

4. Discussion

4.1. Structure. *Coordination Number and Au−S Distances.* Analysis of EXAFS spectra determines a 2-fold coordination of Au complexed by thiosulfate in solution, with a Au−S bond distance of 2.29 Å at 298 K. We first compare this Au−S bond distance in the solution thiosulfate species with other experimentally measured values (Table 1). We are not aware of any previous EXAFS studies of Au complexed by S in solution, which is in part due to the low solubilities of Au(I) thiolate complexes at ambient temperatures. An earlier Au L_{III} EXAFS study of solid sodium gold thiosulfate reported an Au−S bond distance of 2.33 Å.[51] Our EXAFS analysis of solid $Na_3Au(S_2O_3)_2 \cdot 2H_2O$ gives a Au−S distance of 2.28 Å, consistent with the distances of 2.272 and 2.281 Å established from diffraction.[7,39] Au−S distances in compounds with Au coordinated by two S atoms[40] are consistent with the values from our experiment (Table 1). Interestingly, EXAFS has been used to study gold(I) thiomalate and gold(I) thioglucose.[51] These compounds have been used as antiinflammatory drugs in treatments of rheumatoid arthritis for many years, and differ from standard antiinflammatory agents in that they affect chronic rather than acute inflammation. Their mode of action is believed to involve Au interaction with thiol groups in proteins. EXAFS observed Au(I) bound to two S atoms at 2.37 Å in these compounds.[51] These distances, which are longer than the solution Au−S distance of 2.29 Å in $Au(S_2O_3)_2^{3-}$, have been interpreted as arising from polymeric behavior.

We now compare EXAFS and crystallographic data with the structure of gold thiosulfate complex obtained from B3LYP density functional calculations with the effect of solvent modeled by the COSMO dielectric continuum model (Table 4). With the 6-31+G* basis on the ligand atoms and LANL2DZ on the metal, calculated Au−S bond distances are larger than the solution EXAFS distance of 2.29 Å or the 2.27 and 2.28 Å distances found in the crystal, by up to 0.10 Å (Table 4). Increasing the number of Au(I) valence basis functions via the SD+ basis set on gold reduces R(Au−S) by 0.02 Å, modestly improving agreement with experiment (Table 4). We note that a density functional study of the diatomics AuH and Au_2 in vacuo using a B3LYP/LANL2DZ level of theory similarly found bond distances to be overestimated relative to experiment, by 0.04 and 0.10 Å, respectively.[40] These errors increased to 0.06 Å for AuH and 0.13 Å for Au_2 using a MP2/LANL2DZ approach.

Also implicated in gold mobilization,[1] the $Au(SH)_2^-$ complex has a Au−S bond distance of 2.371 Å at the COSMO/B3LYP level of theory with a 6-31+G* basis on the ligands and LANL2DZ on the metal (Table 5), similar to the value of 2.372 Å predicted in $Au(S_2O_3)_2^{3-}$ at this level of theory (Table 4). Increasing the basis on Au(I) again reduces this bond distance by 0.02 Å.

Other Structural Parameters. Although the quality of data for the $Au(S_2O_3)_2^{3-}$ aqueous complex does not allow a multiple-scattering analysis, the similarity of Au−S distances and coordination number between the solid and the complex are consistent with a linear S−Au−S solution complex, as expected from theoretical considerations (Table 4, Figure 3).[3,52] Our calculations find the complexes remain close to linearity at all levels of theory, with an S−Au−S angle of 179.6−179.7°, close to the crystallographic value of 176.5° (Table 4). Similarly, the calculated solution Au−S−S angles agree well with the values of 103.6° and 104.1° observed in the crystal (Table 4). The S−S bond distances are within 0.07−0.09 Å of the crystal EXAFS value (Table 4). Interestingly, all calculations predict a conformation of the thiosulfates approximately antiperiplanar with respect to the dihedral angle $\varphi(S_2-S_1-S_5-S_6)$ (Figure 3), as might be expected from steric arguments. For COSMO/B3LYP/LANL2DZ/6-31+G* stationary structures, the dihedral angle $\varphi(S_2-S_1-S_5-S_6)$ is 178.1°. Employing the SD+ basis on gold, this angle decreases by 2.9° (Table 4). These structures all differ significantly from the conformation observed in the crystal hydrate, where φ of 67° is observed (Table 4), indicative of flexibility in this internal coordinate. This distortion may be a consequence of crystal packing forces.

We turn now to consider structural parameters of the minimum energy geometry of $Au(SH)_2^-$. The S−Au−S ar-

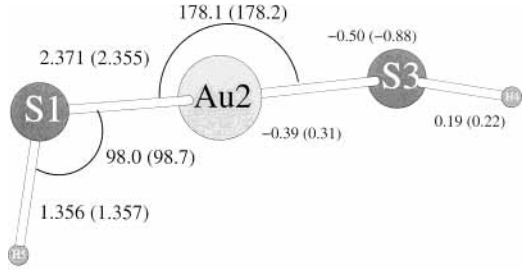

Figure 4. Optimal structure of $Au(SH)_2^-$ at the COSMO/B3LYP/LANL2DZ/6-31+G* level of theory. COSMO/B3LYP/SD+/6-31+G* values are indicated in parentheses. Distances are in Å, angles in deg, and Mulliken charges (using 6-311++G(2df) basis on ligands) in e.

rangement in this complex is also predicted to remain linear in aqueous solution (Table 5, Figure 4). The Au−S−H angles are smaller than the Au−S−S angles of thiosulfate, reflecting the smaller size and charge of the thiolate ligands (Table 5). In contrast to the thiosulfate ligands, the smaller HS^- species form a near-perpendicular H−S−S−H dihedral angle of 81.3° and 83.1° for COSMO/B3LYP/LANL2DZ/6-31+G* and COSMO/B3LYP/SD+/6-31+G* optimal geometries, respectively (Table 5).

Conformational Flexibility. To gain further insight into the difference between calculated and observed crystallographic conformation, we estimate the energetic barrier to rotation about φ, assuming the barrier to exist when the metal−ligand bonds eclipse ($\varphi = 0$). Employing COSMO/B3LYP/LANL2DZ/6-31+G* geometries, the barrier height is estimated to be 2.4 kcal/mol at this level of theory. The barrier height is similar (2.5 kcal/mol) using the COSMO/B3LYP/SD+/6-31+G* geometry and energy. With the larger 6-311++G(2df) basis on the thiosulfate groups, the LANL2DZ energy barrier reduces to 1.8 kcal/mol; however, the SD+ barrier remains almost unchanged at 2.4 kcal/mol. Nonelectrostatic effects contribute less than 0.7 kcal/mol to these predicted barriers. Inspection of Mulliken charges indicates little polarization of the SO_3 moieties or indeed the Au−S bonds on rotation (0.02−0.03 e). Being of the order of *kT*, the energy cost to rotation in solution is readily surmountable at room temperature and is in accord with our solution EXAFS experiments, where rotational averaging makes measurement of distances from the central gold to the central sulfur of the thiosulfate anion impossible. Similarly, rotation about the S−Au−S axis in the crystal permits optimization of intermolecular contacts, with water and with Na^+ counterions. We may conclude that rotation about this axis is unhindered and can adapt readily to environment.

4.2. Stability. Previous studies have indicated that the $Au(S_2O_3)_2^{3-}$ complex forms under mildly reducing to slightly oxidizing conditions, and in neutral to alkaline solutions.[14] This complex may be destabilized by increasing oxygen fugacity (f_{O_2}) as $S_2O_3^{2-}$ is oxidized to $S_4O_6^{2-}$, or by decreasing f_{O_2} as $S_2O_3^{2-}$ is reduced to H_2S and HS^-. By observing decomposition of gold thiosulfate complex at elevated temperature in our EXAFS studies, we have established an approximate upper limit of stability for the gold thiosulfate complex under the conditions of this experiment. We note, however, that increased pH may increase the stability of the thiosulfate anion and in consequence the stability of $Au(S_2O_3)_2^{3-}$.

Theoretically, we can quantify the stability of gold(I) thiosulfate complex via calculation of the bond dissociation energy, as defined in the Methods section (Table 6). Previous studies have indicated a high calculated gold−ligand bond dissociation energy.[53,54] Density functional calculations on Au(I) complexes of neutral ligands in vacuo give large bond dissociation energies ranging from 41.2 kcal/mol for $Au(H_2O)^+$ complex[54] to 95.9 kcal/mol for $Au(PH_3)^+$ complex.[55] Accordingly, our calculations predict a strong metal−S bond in aqueous solution (Table 6). With incorporation of solvent, basis set superposition, and zero-point effects, the Au−S bond dissociation energy is predicted to be 51.4 kcal/mol at the COSMO/B3LYP/LANL2DZ/6-31+G* level, of which 0.4 kcal/mol arises from nonelectrostatic solvent contributions. Basis set superposition error is small (0.8 kcal/mol). At the same geometry but with the split-valence triple-ζ 6-311++G(2df) basis on the ligands, with two sets of d and one set of f polarization functions on S and O atoms, a bond dissociation energy of similar magnitude is observed, of 54.0 kcal/mol (Table 6). Basis set superposition error is again modest (Table 6).

We now consider the effect of augmenting the Au basis: bond dissociation energies increase by 1.0 kcal/mol and remain unchanged using the SD+/6-31+G* and SD+/6-311++G(2df) basis set combinations, respectively, when counterpoise-corrected (ΔE^{BSSE} in Table 6). A BSSE of 0.8 and 2.2 kcal/mol, respectively, is incurred. The larger error for the SD+/6-311++G(2df) basis may reflect a slight basis set imbalance, as isolated metal and ligand species recruit the additional basis functions. However, the BSSE is small relative to the total bond dissociation energy (<5%). Combined with zero-point corrections, we obtain final bond dissociation energies of 52.5 and 53.8 kcal/mol at the COSMO/B3LYP/SD+/6-31+G* and COSMO/B3LYP/SD+/6-311++G(2df) levels of theory, respectively. The significant bond strength in solution correlates with the large overall stability constant for $Au(S_2O_3)_2^{3-}$ ($\beta_{Au,12} \sim 10^{26.1}$) recalculated from measurements in aqueous solution at 298 K.[14]

We turn now to consider bond dissociation energies of $Au(SH)_2^-$ in aqueous solution (Table 7). The Au−S bond strength in $Au(SH)_2^-$ and $Au(S_2O_3)_2^{3-}$ is predicted to be equivalent at the COSMO/B3LYP/LANL2DZ/6-31+G* level of theory. Increasing the ligand basis favors the $Au(S_2O_3)_2^{3-}$ complex. However, subsequently increasing the Au basis leads to prediction of a stronger Au−S bond in $Au(SH)_2^-$ by 0.2 kcal/mol at the COSMO/B3LYP/SD+/6-31+G* level of theory and 0.4 kcal/mol at the COSMO/B3LYP/SD+/6-311++G(2df) level of theory. A dependence on metal and ligand basis is observed similar to $Au(S_2O_3)_2^{3-}$, i.e., a small increase in bond dissociation energy with increased basis, before and after counterpoise correction (Tables 6 and 7). Indeed, for $Au(SH)_2^-$ a small BSSE is once again observed: the largest error, found for the LANL2DZ/6-311++G(2df) basis, is 1.3 kcal/mol (Table 7). We note a previous HF/MIDI! study of $Au(SH)_2^-$ in the gas phase, using a CEP pseudopotential/double-ζ basis for Au, which determined a Au−S bond dissociation energy of 125.5 kcal/mol.[3] Although this energy was obtained via a different theoretical approach, and omitted a BSSE correction, it would appear to suggest that the effect of solvent is to significantly reduce the strength of the Au−S bond in $Au(SH)_2^-$, the result of electrostatic stabilization by water of the ionic dissociation products of the complex.

Previous studies indicate that unusually strong Au−ligand bonds arise from contraction of the 6s orbital due to relativistic effects,[53,54] leading to strong electrostatic interactions and ligand−metal charge transfer. This charge transfer is evidenced in the $Au(S_2O_3)_2^{3-}$ complex by a negative Mulliken charge of −0.61 e on Au(I) at the COSMO/B3LYP/LANL2DZ/6-31+G* level, comparable to a gold(I) Mulliken charge of −0.64 e observed for AuO_2^- in vacuo (bent, end-on binding mode) in a B3LYP/LANL2DZ study.[44] This charge reduces to −0.43 e with

the larger 6-311++G(2df) ligand basis (Figure 3). This is comparable to the value of −0.39 e found on Au in the thiolate complex (Figure 4). A more flexible function space on the metal would appear to yield significantly less ligand−metal charge transfer according to Mulliken population analysis: charges on Au of 0.06 e for $Au(S_2O_3)_2^{3-}$ and 0.31 e for $Au(SH)_2^-$ are obtained from analysis of the respective COSMO/B3LYP/SD+/6-311++G(2df) wave functions. Detailed analysis of Mulliken populations indicates that, for thiolate and thiosulfate complexes, S electron density feeds into empty 6s and 6p orbitals on Au. However, the sensitivity of this electronic structure analysis, to metal basis in particular, suggests caution in its interpretation. Concomitant with rearrangement of electronic distribution on complexation is the change in ligand geometry. Estimates of the deformation energy of each thiosulfate on binding range from 1.2 to 2.8 kcal/mol (Table 6), reflecting the energetic cost of elongating the S−S bond and reducing the S−S−O angle (Supporting Information). By contrast, there is essentially no change in R(S−H) on forming $Au(SH)_2^-$, reflected by a vanishingly small internal energy change (Table 7).

Measurement of the overall stability constant for $Au(SH)_2^-$ in aqueous solution ($\beta_{Au,12} \sim 10^{30.1}$)[1] indicates that $Au(SH)_2^-$ is 4 orders of magnitude more stable than $Au(S_2O_3)_2^{3-}$ in aqueous solution at 298 K, corresponding to a free energy difference of 5.4 kcal/mol. Accordingly, the overall dissociation free energy, calculated at our highest level of theory (COSMO/B3LYP/SD+/6-311++G(2df)) and incorporating thermal and entropic contributions, is 101.4 kcal/mol for $Au(S_2O_3)_2^{3-}$ and 105.8 kcal/mol for $Au(SH)_2^-$ (Table 8). These free energies reflect, within the limits of the harmonic approximation, the larger entropic restriction of the more flexible thiosulfate ligand on complexation. Thus, we predict the thiolate complex to be more stable than gold(I) thiosulfate in aqueous solution at all levels of theory, the preference ranging from 1.0 to 4.4 kcal/mol (Table 8). At the highest level, a difference of 4.4 kcal/mol is calculated, which is in good agreement with an experimental value of 5.4 kcal/mol (Table 8). As Au(I) is a soft Lewis acid, the increased stability of the thiolate has been connected with increased softness of the ligating S atom, relative to thiosulfate.[1] The stability of gold thiolate complexes in reducing conditions (Au(SH) and $Au(SH)_2^-$, depending on pH) have also been measured under P/T conditions of up to 673 K and 1500 bar, and are strongly suggestive of gold transported as thiolate complex in high-temperature geothermal fluids.[2] Under more oxidizing conditions, thiosulfate can be recruited to mobilize aurous gold. Our theoretical and experimental observations are in accord with this scheme of Au transport, further emphasizing the important role of thio gold(I) complexes in mobilization of gold in geothermal fluids.

5. Conclusion

In this investigation, we have examined aqueous solutions of $Au(S_2O_3)_2^{3-}$ complexes using EXAFS and high level density functional quantum mechanical calculations. The structural environment of Au in the gold thiosulfate complex, determined by EXAFS analysis of Au L_{III} edge fluorescence spectra taken at 298 and 348 K on an ultradilute EXAFS beam line, shows Au(I) coordinated by two sulfurs at 2.29 Å. Quantum mechanical calculations predict a linear S−Au−S geometry, and are further employed to predict the aqueous solution conformation of the complex, which is found to differ significantly from the crystallographic geometry. The corresponding conformational barrier to internal rotation of the complex in solution is low (<3 kcal/mol). For this reason, it is not unexpected to observe in the crystal a deviation of 108° from the calculated solution structure of $Au(S_2O_3)_2^{3-}$. The calculated solution Au−S bond dissociation energy in $Au(S_2O_3)_2^{3-}$ is estimated to be 53.8 kcal/mol from density functional theory and is large, as expected from strong relativistic effects associated with Au(I).[55] The associated basis set superposition error is small, constituting less than 5% of the total bond dissociation energy. With increased ligand and metal basis set, we find a general increase in the relative preference of $Au(SH)_2^-$ over $Au(S_2O_3)_2^{3-}$ with respect to Au−S bond dissociation energy. Ligand−metal charge transfer occurs on complexation, although the extent from analysis is sensitive to basis set. Our highest level calculations also indicate that the thio complex, $Au(SH)_2^-$, is 4.4 kcal/mol more stable in free energy than $Au(S_2O_3)_2^{3-}$, in accord with a value of 5.4 kcal/mol calculated from reported stability constants for these species. In our experiments, we observe decomposition of the $Au(S_2O_3)_2^{3-}$ complex at temperatures at 393 K. This observation suggests that thermal instability of this complex may restrict the temperature range over which Au(I) can be transported by thiosulfate, in contrast to the thiolate complex which can transport gold at elevated temperatures and pressures.

Subsequent to metal transport, breakdown of $Au(S_2O_3)_2^{3-}$ is required for release of gold. The mechanisms for this process remain unclear. Recent studies have shown thio Au complexes to strongly absorb onto sulfide mineral surfaces, including antimony, arsenic, and iron sulfides.[56−58] Adsorption of hydrosulfidogold(I) complexes by iron sulfide phases is pH dependent, and thus Au−S species dependent.[58] Here, the main gold complex adsorbed is Au(SH); adsorption of $Au(SH)_2^-$ onto negatively charged sulfide surfaces is not favored. Chemisorption of thio Au complexes onto FeS (mackinawite) leads to reduction of Au(I) solution complexes to Au(0) and to formation of surface polysulfides.[58] Few studies, however, have addressed absorption of gold thiosulfate complexes onto minerals.[59] Thus, further research via spectroscopic and computational approaches is required to address possible mechanisms of gold thiosulfate absorption onto surfaces. Such studies will enhance our understanding of Au mobilization and deposition occurring under ore-forming conditions.

Acknowledgment. We are grateful to NERC for a ROPA award (GR3/R9926). We acknowledge Bob Bilsborrow, Fred Mosselmans, and the director and the staff of the SRS for their help during our experiments at The Daresbury Laboratory. R.A.B. gratefully acknowledges a Ramsay Fellowship.

Supporting Information Available: Tables 1S−8S listing calculated stationary structures for thiosulfate and complexes. This material is available free of charge via the Internet at http://pubs.acs.org.

References and Notes

(1) Renders, P. J.; Seward, T. M. *Geochim. Cosmochim. Acta* **1989**, *53*, 245.
(2) Benning, L. G.; Seward, T. M. *Geochim. Cosmochim. Acta* **1996**, *60*, 1849.
(3) Tossell, J. A. *Geochim. Cosmochim. Acta* **1996**, *60*, 17.
(4) Tykodi, R. J. *J. Chem. Educ.* **1990**, *67*, 146.
(5) Elerman, Y.; Fuess, H.; Joswig, W. *Acta Crystallogr., Sect. B* **1982**, *B38*, 1799.
(6) Cavalca, L.; Mangia, A.; Palmieri, C.; Pelizzi, G. *Inorg. Chim. Acta* **1970**, 299.
(7) Baggio, R. F.; Baggio, S. *J. Inorg. Nucl. Chem.* **1973**, *55*, 3191.
(8) Gasparri, G. F.; Mangia, A.; Musatti, A.; Nardelli, M. *Acta Crystallogr., Sect. B* **1968**, *B25*, 203.
(9) Nardelli, M.; Fava, G. *Acta Crystallogr.* **1962**, *15*, 477.
(10) Webster, J. G. *Appl. Geochem.* **1987**, *2*, 579.

(11) Xu, Y.; Schoonen, M. A. A.; Nordstrom, D. K.; Cunningham, K. M.; Ball, J. W. *J. Volcanol. Geotherm. Res.* **2000**, *97*, 403.
(12) Xu, Y.; Schoonen, M. A. A. *Geochim. Cosmochim. Acta* **1995**, *59*, 4605.
(13) Jorgensen, B. B. *Science* **1990**, *249*, 152.
(14) Webster, J. G. *Geochim. Cosmochim. Acta* **1986**, *50*, 1837.
(15) Klamt, A.; Schuurmann, G. *J. Chem. Soc., Perkin Trans. 2* **1993**, 799.
(16) Lennie A. R.; Charnock, J. M.; Pattrick, R. A. D. *Chem. Geol.* **2003**, in press.
(17) Binsted, N. *EXCURV98*; CCLRC Daresbury Laboratory Computer Program 1998.
(18) Gurman, S. J.; Binsted, N.; Ross, I. *J. Phys. C* **1984**, *17*, 143.
(19) Gurman, S. J.; Binsted, N.; Ross, I. *J. Phys. C* **1986**, *19*, 1845.
(20) Binsted, N.; Strange, R. W.; Hasnain, S. S. *Biochemistry* **1992**, *31*, 12117.
(21) Hay, P. J.; Wadt, W. R. *J. Chem. Phys.* **1985**, *82*, 270.
(22) Dunning, T. H.; Hay, P. J. In *Modern Theoretical Chemistry*; Schaefer, H. F., III, Ed.; Plenum: New York, 1976.
(23) Hemmingsen, L.; Amara, P.; Ansoborlo, E.; Field, M. J. *J. Phys. Chem. A* **2000**, *104*, 4095.
(24) Becke, A. D. *J. Chem. Phys.* **1993**, *98*, 5648.
(25) Lee, C.; Yang, W.; Parr, R. G. *Phys. Rev. B* **1988**, *37*, 785.
(26) Andrae, D.; Haussermann, U.; Dolg, M.; Stoll, H.; Preuss, H. *Theor. Chim. Acta* **1990**, *77*, 123.
(27) Schwerdtfeger, P.; Dolg, M.; Schwarz, W. H. E.; Bowmaker, G. A.; Boyd, P. D. W. *J. Chem. Phys.* **1989**, *91*, 1762.
(28) Hehre, W. J.; Ditchfield, R.; Pople, J. A. *J. Chem. Phys.* **1972**, *56*, 2257.
(29) McLean, A. D.; Chandler, G. S. *Chem. Phys. Lett.* **1980**, *76*, 163.
(30) Boys, S. F.; Bernardi, F. *Mol. Phys.* **1970**, *19*, 553.
(31) Hehre, W. J.; Radom, L.; Schleyer, P. v. R.; Pople, J. A. *Ab initio molecular orbital theory*; J. Wiley & Sons: New York, 1986.
(32) Floris, F. M.; Tomasi, J.; Ahuir, J. L. P. *J. Comput. Chem.* **1991**, *12*, 784.
(33) Huron, M. J.; Claverie, P. *J. Phys. Chem.* **1972**, *76*, 2123.
(34) Rappe, A. K.; Casewit, C. J.; Colwell, K. S.; Goddard, W. A., III; Skiff, W. M. *J. Am. Chem. Soc.* **1992**, *114*, 10024.
(35) Barone, V.; Cossi, M.; Tomasi, J. *J. Chem. Phys.* **1997**, *107*, 3210.
(36) Marcus, Y. *J. Chem. Soc., Faraday Trans.* **1991**, *87*, 2995.
(37) Bondi, A. *J. Phys. Chem.* **1964**, *68*, 441.
(38) Frisch, M. J.; Trucks, G. W.; Schlegel, H. B.; Scuseria, G. E.; Robb, M. A.; Cheeseman, J. R.; Zakrzewski, V. G.; Montgomery, J. A.; Stratmann, R. E.; Burant, J. C.; Dapprich, S.; Millam, J. M.; Daniels, A. D.; Kudin, K. N.; Strain, M. C.; Farkas, O.; Tomasi, J.; Barone, V.; Cossi, M.; Cammi, R.; Mennucci, B.; Pomelli, C.; Adamo, C.; Clifford, S.; Ochterski, J.; Petersson, G. A.; Ayala, P. Y.; Cui, Q.; Morokuma, K.; Malick, D. K.; Rabuck, A. D.; Raghavachari, K.; Foresman, J. B.; Cioslowski, J.; Ortiz, J. V.; Baboul, A. G.; Stefanov, B. B.; Liu, G.; Liashenko, A.; Piskorz, P.; Komaromi, I.; Gomberts, R.; Martin, R. L.; Fox, D. J.; Keith, T. A.; Al-Laham, M. A.; Peng, C. Y.; Nanayakkara, A.; Gonzalez, C.; Challacombe, M.; Gill, P. M. W.; Johnson, B. G.; Chen, W.; Wong, M. W.; Andres, J. L.; Head-Gordon, M.; Replogle, E. S.; Pople, J. A. *Gaussian 98*; Gaussian, Inc.: Pittsburgh, PA, 1998.
(39) Ruben, H.; Zalkin, A.; Faltens, M. O.; Templeton, D. H. *Inorg. Chem.* **1974**, *13*, 1836.
(40) Bishop, P.; Marsh, P.; Brisdon, A. K.; Brisdon, B. J.; Mahon, M. F. *J. Chem. Soc., Dalton Trans.* **1998**, 675.
(41) Legge, F. S.; Nyberg, G. L.; Peel, J. B. *J. Phys. Chem. A* **2001**, *105*, 7905.
(42) Tossell, J. A. *Chem. Geol.* **1997**, *141*, 93.
(43) Vincent, M. A.; Palmer, I. J.; Hillier, I. H.; Akhmatskaya, E. *J. Am. Chem. Soc.* **1998**, *120*, 3431 and references therein.
(44) Okumura, M.; Kitagawa, Y.; Haruta, M.; Yamaguchi, K. *Chem. Phys. Lett.* **2001**, *346*, 163.
(45) Hotop, H.; Lineberger, W. C. *J. Phys. Chem. Ref. Data* **1988**, *14*, 731.
(46) Galbraith, J. M.; Schaefer, H. F., III *J. Chem. Phys.* **1996**, *105*, 862.
(47) Brown, S. T.; Rienstra-Kiracofe, J. C.; Schaefer, H. F., III *J. Phys. Chem. A* **1999**, *103*, 4065.
(48) *CRC Handbook of Chemistry and Physics*; Lide, D. R., Ed.; CRC Press: Boca Raton, FL, 1997.
(49) Trasatti, S. *Pure Appl. Chem.* **1986**, *58*, 955.
(50) Maw, S. A.; Bryce, R. A.; Hall, R. J.; Masters, A. J.; Hillier, I. H. *J. Phys. Chem. B* **1998**, *102*, 4089.
(51) Mazid, M. A.; Razi, M. T.; Sadler, P. J.; Greaves, G. N.; Gurman, S. J.; Koch, M. H. J.; Phillips, J. C. *J. Chem. Soc., Chem. Commun.* **1980**, 1261.
(52) Puddephatt, R. J. In *Comprehensive Coordination Chemistry*; Wilkinson, G.; Ed.; Pergamon: Oxford, 1987; Vol. 5.
(53) Hertwig, R. H.; Koch, W.; Schroder, D.; Schwarz, H.; Hrusak, J.; Schwerdtfeger, P. *J. Phys. Chem.* **1996**, *100*, 12253.
(54) Schroder, D.; Schwarz, H.; Hrusak, J.; Pyykko, P. *Inorg. Chem.* **1998**, *37*, 624.
(55) Häberlen, O. D.; Rösch, N. *J. Phys. Chem.* **1993**, *97*, 4970.
(56) Renders, P. J.; Seward, T. M. *Geochim. Cosmochim. Acta* **1989**, *53*, 255.
(57) Cardile, C. M.; Cashion, J. D.; McGrath, A. C.; Renders, P. J.; Seward, T. M. *Geochim. Cosmochim. Acta* **1993**, *57*, 2481.
(58) Widler, A. M.; Seward, T. M. *Geochim. Cosmochim. Acta* **2002**, *66*, 383.
(59) Machesky, M. L.; Andrade, W. O.; Rose, A. W. *Geochim. Cosmochim. Acta* **1991**, *55*, 769.